

Toxicity of biosynthetic silver nanoparticles on the growth, cell ultrastructure and physiological activities of barley plant

K. A. Fayez^{1,2} · B. A. El-Deeb^{1,2} · N. Y. Mostafa^{1,3}

Received: 4 July 2016/Revised: 10 June 2017/Accepted: 17 June 2017/Published online: 27 June 2017
© Franciszek Górski Institute of Plant Physiology, Polish Academy of Sciences, Kraków 2017

Abstract Silver nanoparticles (AgNPs) were biosynthesized using the cell-free filtrate of bacterium *Proteus mirabilis*, reacted with 1 mM of AgNO₃ solutions at 37 °C. The synthesis of AgNPs was monitored by UV–Vis spectroscopy and transmission electron microscopy (TEM) equipped with selected area electron diffraction (SAED). The results point to formation of spherical to cubical particles of AgNPs ranging in size from 5 to 35 nm with an average of 25 nm in diameter. The toxicity of Ag on barley (*Hordeum vulgare* L. cv. Gustoe) that was subjected to Ag⁺ as AgNO₃ and AgNPs was explored. The grain germination and seedling growth of barley decreased in the presence of 0.1 mM Ag⁺ and was inhibited at 1 mM Ag⁺. In contrast, our results indicated that the AgNPs at low concentration (0.1 mM) could be useful for barley grain germination and seedling growth. However, the higher concentrations of AgNPs (0.5 and 1 mM) reduced grain germination and exhibited a stronger reduction in the root length. A decline in the photosynthetic pigments and disorganization of chloroplast grana thylakoids in Ag⁺ and AgNPs-treated plants confirmed the leaf chlorosis. An increase of plastoglobuli within chloroplasts was observed in Ag⁺ and AgNPs-treated leaves. Ag⁺ caused dense

aggregation of nuclear chromatin materials and degeneration of mitochondria. Ag⁺ and AgNPs increased contents of malondialdehyde, soluble proteins, total phenolic compounds and activity of guaiacol peroxidase in barley leaves; these results point to activation of plant defence mechanisms against oxidative stress in barley.

Keywords *Hordeum vulgare* · *Proteus mirabilis* · Silver nanoparticles · Ultrastructure · Oxidative stress · Metabolites · Peroxidase

Abbreviations

Chl	Chlorophyll
MDA	Malondialdehyde
NPs	Nanoparticles
POX	Peroxidase
ROS	Reactive oxygen species
SAED	Selected area electron diffraction
TBA	Thiobarbituric acid

Introduction

Nanotechnology applications play an important role in medicine, biology, industry, food and cosmetics (Fabrega et al. 2011; Kokura et al. 2010; McGillicuddy et al. 2017; Nel et al. 2006; Tiede et al. 2008). Nanoparticles (NPs) are materials with a minimum of two dimensions ranging in size between 1 and 100 nm (American Society for Testing and Materials 2006; Hood 2004). NPs were produced via chemical and physical procedures for several decades and recently, the biosynthesis and effect of NPs on plants has been studied (Gurunathan et al. 2009; Krishnaraj et al. 2012). Uptake, transport, accumulation and the interactions of NPs with plants and biotic constituents of the

Communicated by A. Krolicka.

✉ K. A. Fayez
khalaffayez@yahoo.com

¹ Biology Department, Faculty of Science, Taif University, Al-Haweiah, P.O. Box 888, 21974 Taif, Saudi Arabia

² Botany Department, Faculty of Science, Sohag University, Sohag, Egypt

³ Chemistry Department, Faculty of Science, Suez Canal University, Ismailia, Egypt

environment were reported (Battke et al. 2008; Doshi et al. 2008; Impellitteri et al. 2009; Lin and Xing 2007). So, accumulation of NPs in the environment and its release (transversion) to ions is expected.

Among nanoparticles, AgNPs are the most metallic nanoparticles used in consumer products (Godin et al. 2010; Klaine et al. 2008; Marambio-Jones and Hoek 2010; Pal et al. 2007). The accumulation and effect of NPs on plants depend on their physical and chemical properties as well as on the constituents of subcellular sites of NPs deposition (Dietz and Herth 2011). Ag⁺ and silver NPs reduced growth, photosynthetic pigment synthesis and caused severe damage in metabolism of plants (Cvjetko et al. 2017; Mazumdar and Ahmed 2011; Miao et al. 2009). Disturbance cell division of *Allium cepa* root tip (Kumari et al. 2009), and damaged root epidermis and root cap of *Lolium multiflorum* (Yin et al. 2011) were reported in response to AgNPs effect. Compared with bulk Ag, AgNPs were reduced biomass and transpiration of *Cucurbita pepo* by 66–84% (Musante and White 2012). On the other hand, low concentration of AgNPs extended the vase life and increased antioxidant enzyme activities of cut rose flowers (Hassan et al. 2014). However, pulse treatment for 1 h in high concentration of AgNPs (250 mg/L) had toxicity effect on cut rose flowers (Lü et al. 2010).

Enhanced reactive oxygen species (ROS) generation due to release Ag⁺ from AgNPs interacted with various cell components and induced oxidative stress (Gorczyca et al. 2015; Haverkamp and Marshall 2009; Kim et al. 2007; Kumar and Yadav 2009; Nair and Chung 2014; Pal et al. 2007). AgNPs toxicity on nitrifying bacteria confirmed that ROS had significant role in the cell response to NPs (Choi and Hu 2008). Moreover, numerous of other than ROS factors, which control the toxicity of silver nanoparticles were identified (Chairuangkitti et al. 2013; Dubey et al. 2015; Yuan et al. 2013). AgNPs are toxic to plant seedlings and reduced algal photosynthetic yield (Navarro et al. 2008a). Moreover, phytotoxicity of AgNPs on *Chlamydomonas reinhardtii* algal cells was more toxic than Ag⁺ (Navarro et al. 2008b). AgNPs altered the transcription of antioxidant and aquaporin genes, and changed the balance between the oxidant and antioxidant systems in *Arabidopsis thaliana* (Qian et al. 2013).

The present study aims to compare the influence of AgNO₃ and biosynthetic AgNPs on grain germination, seedling growth, cell ultrastructure, photosynthetic pigments, total soluble proteins and carbohydrate, total phenolic compounds, lipid peroxidation and peroxidase activity in barley leaves.

Materials and methods

Biosynthesis of Silver nanoparticles

Biosynthesis of silver nanoparticles was carried out according to Bhainsa and D'Souza (2006) with some modifications. To obtain stable silver nanoparticles, the bacterium *Proteus mirabilis* was grown in a 500 mL Erlenmeyer flask containing nutrient broth (5 g peptone, 3 g yeast extract and 5 g NaCl/L). The flasks were incubated for 24 h in a shaker set at 120 rpm and 28 °C. After the incubation period, the culture was centrifuged at 10,000×g (Table Top Refrigerated Centrifuge Z 36 HK, Germany) and about 0.5 g of wet biomass of bacterium *P. mirabilis* was brought into contact with 100 mL sterile double-distilled water for 48 h at 28 °C in a 250 mL Erlenmeyer flask and was shaken at 200 rpm. After incubation, the cell-free filtrate was obtained by centrifugation. The cell-free filtrate was used for synthesis of silver nanoparticles. For silver nanoparticles biosynthesis, the silver nitrate was mixed with 100 mL of cell-free filtrate in a 250 mL Erlenmeyer flask to obtain a final concentration of 1 mM silver ions. The mixture was incubated at 37 °C for 24 h in dark. AgNPs was checked by visual observation of the color from light-yellow to brown and by measurement of the UV–Vis spectra. To confirm the purity, stability and complete conversion of Ag⁺ to AgNPs, the AgNPs solution was centrifuged at 15,000×g for 30 min. The clear supernatant was tested using NaCl solution and spectrophotometer. Both tests revealed no Ag⁺ remained in the supernatant. Three months after biosynthesis of AgNPs, and at room temperature, AgNPs has the same spectra confirmed its stability. Nutrient Agar plates test confirmed no microbial contamination in the AgNPs solution.

Characterization of silver nanoparticles

Ultraviolet–visible spectroscopy (UV–Vis) was performed in a PerkinElmer Lambda spectrophotometer. Size, morphology and composition of the nanoparticles were studied by observation in transmission electron microscopy (TEM) operated at 220 kV accelerating voltage (Jeol-2100 Japan) equipped with selected area electron diffraction (SAED) at Egyptian Petroleum Research Institute, Egypt. TEM samples were prepared by placing drops of the silver nanoparticles solution on carbon-coated TEM grids. The obtained images were processed using the software ImageJ. ImageJ developed at the National Institutes of Health (NIH), USA, is a Java-based public domain image processing and analysis program (Rasband 1997).

Plant experiments

Germination of barley

Barley grains (*Hordeum vulgare* L. cv. Gustoe) were surface sterilized with 5% sodium hypochlorite solution for 10 min and then carefully washed several times with distilled water to remove the sodium hypochlorite. Sterilized barley grains were germinated on moist filter paper in Petri-dishes containing 10 mL solution of each concentration of AgNO₃ and AgNPs (0, 0.1, 0.5 and 1 mM), as well as the control (distilled water) for 1 week. The different solutions of AgNO₃ and AgNPs as well as the control were renewed two times during the experiment period of germination (1 week). Each treatment was made in three replicates (each replicate is one Petri dish containing 10 barley grains). Barley grains germination index under different treatments were calculated using the formula; germination index (G.I.) = (no. of grains germinated/total no. of grains) × 100. The length of seedling shoot was estimated under control and treated plants.

Cultivation of barley

In the second experiment, barley grains were surface sterilized with 5% sodium hypochlorite solution for 10 min and carefully washed several times with distilled water. Grains were sown in appropriate clean plastic pots containing 200 g of soil composed of clay and sand at 1:2 (v/v ratio). The experiment soil had pH = 7.36; electrical conductivity (EC) = 1.05 dS/m; and 0.65 g of total dissolved salts/L. The soil available Na⁺ and K⁺ were 19 and 42 ppm, respectively. All pots were watered up to 85% of the soil water content (SWC) with distilled water. The levels of soil water content (85%) were controlled by weighing the pots every two days. The soil water content (SWC) was calculated according to the following equation: [(wet soil – dry soil)/dry soil] × 100. The wet and dry soils are the weight of soil after water drainage and oven dried soil, respectively.

Two weeks after sowing of grains, plants were randomly divided into five groups. The identification of plant group treatments was as follows: group 1, untreated plant (control); groups 2 and 3, plants treated with two levels of AgNO₃ (0.5 and 1 mM, respectively); groups 4 and 5, plants treated with two levels of AgNPs (0.5 and 1 mM, respectively). Each treatment was made in three replicates (each replicate is one pot containing 20 seedlings). The treated and untreated plants were grown for 3 weeks in open field under natural light conditions (≈ 14 h light: 10 h dark) during the growing season of barley. Leaf samples were collected separately from the control, AgNO₃ and AgNPs-treated barley in three replicates. Leaf morphology,

mesophyll cell ultrastructure, photosynthetic pigment contents, malondialdehyde contents, protein contents, phenolic compounds and guaiacol peroxidase activity of the control, Ag⁺ and AgNPs-treated barley leaves were estimated.

Determination of silver

Leaves of barley plants were collected and dried at 60 °C for 3 days. The samples were digested by using a microwave system CEM Mars 5 (CEM Corporation, Matthews, NC USA). Each sample was transferred to a freshly cleaned and rinsed microwave digestion vessel. Then 5 mL nitric acid, 1 mL hydrochloric acid and 0.5 mL hydrogen peroxide (30%) was added and the samples were digested in the microwave oven. Then samples were ramped to 180 °C for 20 min and held at 180 °C for 10 min before cooling to below 50 °C. Prior to analysis the digests, sample preparation blanks and calibrate were diluted appropriately. All chemicals used were of analytical grade. Nitric acid, hydrochloric acid and hydrogen peroxide were purchased from Merck, Darmstadt, Germany. Calibration standard solutions of silver were made of a certified standard single element stock solution from PerkinElmer (Silver Pure Single-Element Standard, 1000 mg/L, 2% HNO₃, 500 mL). Deionized water was purified by a Millipore system (Milli-Q, 18.2 MΩcm).

In the present study, the concentration of Ag in the digested leaf solution was determined by inductively coupled plasma optical emission spectrometer (ICP-OES with the PerkinElmer Optima 2100DV). Calibration of ICP-OES was done using a certified silver standard solution from PerkinElmer (Silver Pure Single-Element Standard 1000 mg/L), which was serially diluted to prepare calibrate solutions. The quantification was carried out by external three-point-calibration. Stock solutions were diluted with approximately 0.5% HCl to relevant concentration levels.

Leaf morphology and cell ultrastructure

For symptom and morphological changes, the leaves of control and treated plants with 0.5 and 1 mM of AgNO₃ and AgNPs concentrations were photographed. For ultrastructure studies, fresh leaves (1–2 mm) were fixed for 3 h in 3% glutaraldehyde prepared in 0.05 M phosphate buffer (pH 7). Samples were rinsed several times in 0.05 M phosphate buffer and then were post fixed with 1% OsO₄ in 0.05 M phosphate buffer for 2 h. Samples were rinsed several times with 0.05 phosphate buffer and then dehydrated in a gradient ethanol series and embedded in Epon-812 (Luft 1961). Ultrathin sections (60–70 nm thick) were stained with uranyl acetate and lead citrate. Specimens were viewed with Jeol-1010 transmission electron

microscope (Unit of Electron Microscopy at Sohag University, Egypt; and Taif University, Saudi Arabia) at 80 kV.

Determination of photosynthetic pigments

Contents of chlorophyll *a* (Chl *a*), chlorophyll *b* (Chl *b*) and total carotenoids (Car) were spectrophotometrically (Jenway 6300 spectrophotometer, UK) determined according to Lichtenthaler (1987). The photosynthetic pigment content was extracted from a known fresh weight of leaves in 85% (v/v) aqueous acetone. The extract was centrifuged at $4000\times g$ for 10 min. The absorbance was measured against a blank of pure 85% aqueous acetone at three wavelengths 663, 647 and 470 nm according the following equations:

$$\text{Chla} = 12.25 A_{663} - 2.79 A_{647}$$

$$\text{Chlb} = 21.50 A_{647} - 5.10 A_{663}$$

$$\text{Car} = (1000 \times A_{470} - 1.82 \times \text{Chl } a - 95.15 \times \text{Chl } b) / 225$$

The pigment contents (Chl*a*, Chl*b* and carotenoids) were calculated as mg g^{-1} FW.

Determination of malondialdehyde

Malondialdehyde (MDA) content was estimated according to Hernández and Almansa (2002). Fresh leaf samples (500 mg) were homogenized in 5 mL 0.1% trichloroacetic acid (TCA). The homogenate was centrifuged at $15,000\times g$ for 20 min at 4 °C. One mL aliquot of the supernatant was mixed with 3 mL 0.5% thiobarbituric acid (TBA) prepared in 20% TCA and incubated at 90 °C for 20 min. After stopping the reaction in an ice bath, samples were centrifuged at $10,000\times g$ for 5 min. The supernatant absorbance at 532 nm was measured. After subtracting the non-specific absorbance at 600 nm, MDA concentration was determined using the extinction coefficient $155 \text{ mM}^{-1} \text{ cm}^{-1}$.

Determination of soluble proteins and total phenolic compounds

Leaf soluble proteins content was determined according to Lowry et al. (1951). Samples (0.1 g DW) were extracted in 10 mL distilled water for 2 h at 90 °C. The extracts were centrifuged and the supernatants were collected. One mL of extract was added to 5 mL of alkaline reagent (50 mL 2% Na_2CO_3 prepared in 0.1 N NaOH and 1 mL 0.5% $\text{CuSO}_4 \cdot 5\text{H}_2\text{O}$ prepared in 1% sodium potassium tartarate) mixed thoroughly and then allowed to stand for 10 min. A total of 0.5 mL Folin-Ciocalteu reagent diluted 1:2 (v/v) was then added and mixed immediately. After 30 min, the extinction against appropriate blank was measured at

700 nm. Bovine serum albumin was used as a standard. Protein contents were expressed as mg g^{-1} DW.

Total phenolic was measured according to Dai et al. (1994). Twenty-five microliter of the extract was mixed with 110 μL Folin-Ciocalteu reagent, 200 μL 20% sodium carbonate and 1.9 mL distilled water and placed at 60 °C for 30 min. Optical density was measured with a spectrophotometer at 750 nm. A standard curve was constructed with different concentrations of gallic acid. The results were expressed as μg of gallic acid g^{-1} DW.

Peroxidase activity (POX)

POX (EC 1.11.1.7) activity was measured by the following change in the absorption due to guaiacol oxidation ($E = 26.1 \text{ mM}^{-1} \text{ cm}^{-1}$) at 470 nm according to Polle et al. (1994). The activity was assayed for 1 min in a reaction solution (3 mL final volume) composed of 100 mM potassium phosphate buffer (pH 7.0), 20 mM guaiacol, 10 mM H_2O_2 and 50 μL of crude extract. Enzyme activity was calculated in terms of μM of guaiacol oxidized $\text{min}^{-1} \text{ g FW}$.

Statistical analysis

The data were tested for significance by using one-way of variance (ANOVA) test. Means were compared by least significant differences (LSD) test at levels $P < 0.05$ and $P < 0.01$. The statistical tests were carried out using SPSS 9.0 statistical software for Windows.

Results and discussion

Synthesis and characterization of AgNPs

In this study, bacterium *Proteus mirabilis* was used for the biosynthesis of silver nanoparticles as stated in materials and methods. Biological silver nanoparticles are being extensively synthesized using various organisms (Rajan et al. 2015; Shaligram et al. 2009; Shivaji et al. 2011). The biosynthesis of AgNPs was confirmed by UV–Vis spectroscopy measurements of the reaction medium. After the AgNO_3 solution has reacted with the cell-free filtrate, a clear brown homogenous suspension of AgNPs formed. The absorption band at about $\sim 430 \text{ nm}$ (Fig. 1a) is a characteristic feature of spherical AgNPs attributed to the surface Plasmon resonance of AgNPs obtained from the reaction mixture of cell-free filtrate of *Proteus mirabilis* with AgNO_3 which was absent in the control. The absorption band was sharp, which indicates little aggregation of nanoparticles in the solution. Resonance band of

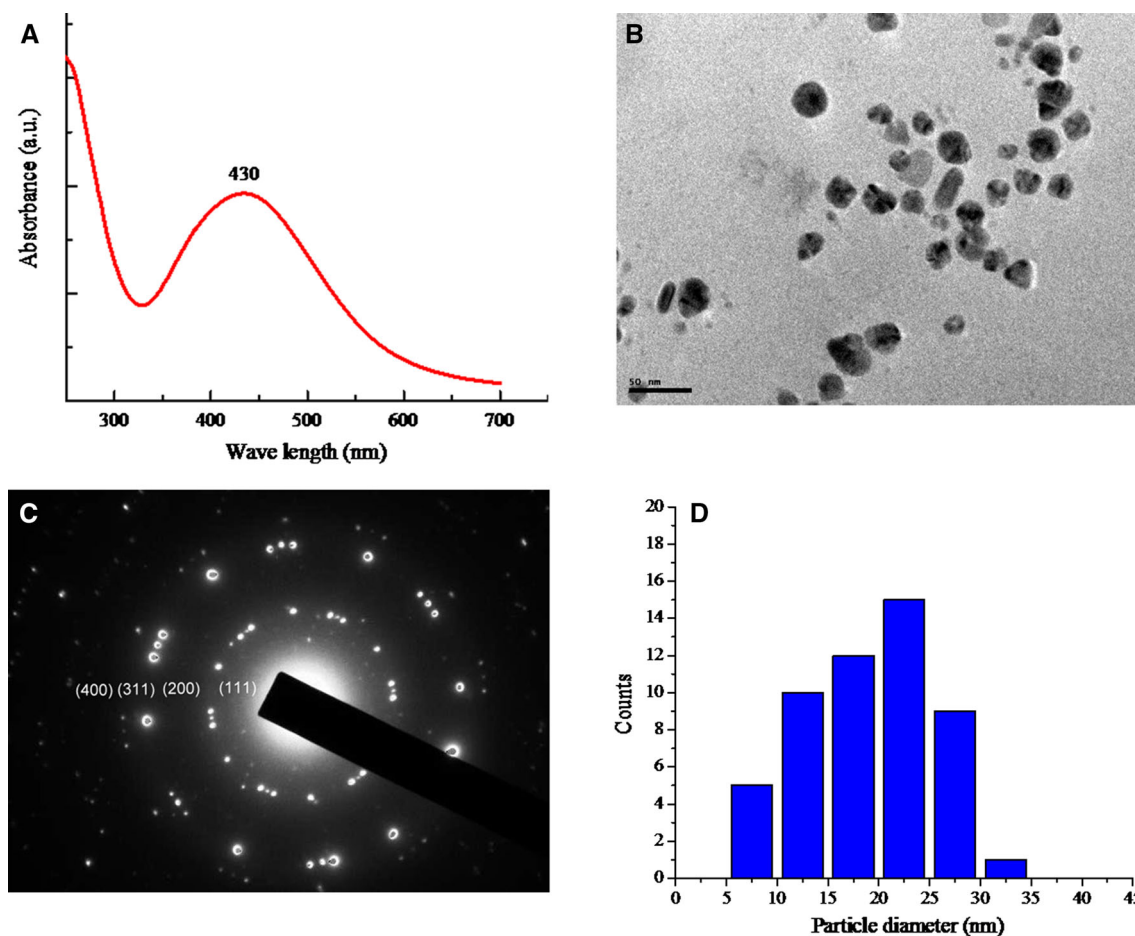


Fig. 1 Characterization of the AgNPs synthesized from AgNO_3 using cell-free filtrate of *Proteus mirabilis*; UV-Visible spectra (a), TEM image of AgNPs (b), SAED image (c) and particle size distributions (d)

AgNPs was reported around this region (Al-Harbi et al. 2014; Raut et al. 2010). However, the exact position is depending on the particle size, substance surrounding, adsorbed species on the surface and dielectric constant (Amooghaie et al. 2015; Mulvaney 1996; Sharma et al. 2009).

TEM image (Fig. 1b) described the size and shape of the biosynthesized silver nanoparticles with their respective selected area electron diffraction (SAED) pattern (Fig. 1c) and particle diameter (Fig. 1d). The SAED pattern (Fig. 1c) of silver particles was carried out on polycrystalline showed only some spots of diffraction distributed on concentric circles. The rings patterns with plane distances 2.37, 2.05, 1.44 and 1.02 Å were consistent with the plane families (111), (200), (311) and (400) of pure face-centered cubic (fcc) silver crystal structure. Different sizes of particles ranging from 5 to 35 nm in diameter, poly dispersed, small and large spherical to cubical shape were formed. The enlarged TEM image revealed almost 25% of the silver nanoparticles were 25 nm in diameter (Fig. 1d).

Grain germination and seedling growth

The toxicity effect of Ag^+ and AgNPs on barley grain germination and seedling growth was evaluated (Fig. 2). The effect of silver as Ag^+ on barley grain germination, shoot and root lengths was more evident than that of AgNPs. Ag^+ (0.1, 0.5 and 1 mM) treatments had a clear effect on barley grain germination and seedling growth compared to the corresponding concentrations of AgNPs treatments and to the control (Fig. 2; Table 1). Under effect of 0.1 and 0.5 mM Ag^+ , the grain germination was 84 and 49.7% of the control, respectively, and was inhibited at 1 mM Ag^+ . Shoot length decreased by 26.1 and 81.8% in response to 0.1 and 0.5 mM Ag^+ , respectively. On the other hand, the toxicity of Ag^+ on root length was more pronounced than shoot (Fig. 2).

Compared to the control, the 0.1 mM AgNPs treatment caused an increase in shoot and root lengths of barley seedling, this increase may be attributed to enhancement some enzyme activities (Fig. 2). However, AgNPs at 0.5 and 1 mM decreased root and shoot lengths, with a more

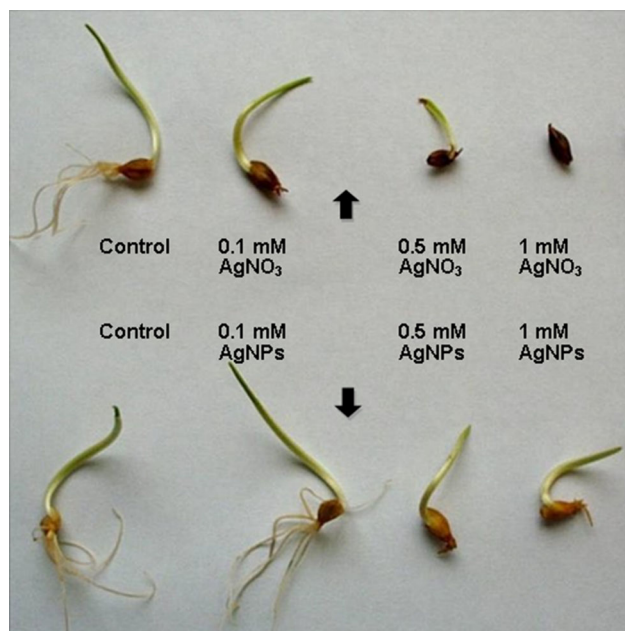


Fig. 2 Germination and seedling lengths of barley grains (*Hordeum vulgare* L. cv. Gustoe) treated with three concentrations of AgNO_3 and AgNPs (0.1, 0.5 and 1 mM) for 1 week

Table 1 Grain germination (%) and seedling shoot length (cm) of barley (*Hordeum vulgare* L. cv. Gustoe) treated with Ag^+ or AgNPs (0.1, 0.5 and 1 mM) for 1 week compared to the control

Treatments	Grain germination (%) M \pm SD	Shoot length (cm)	
		M \pm SD	%
Control	90.9 \pm 1.05	5.86 \pm 0.28	100
0.1 mM AgNO_3	76.4** \pm 1.38	4.33** \pm 0.21	73.9
0.5 mM AgNO_3	45.2** \pm 1.49	1.61** \pm 0.17	18.2
1.0 mM AgNO_3	00.0** \pm 0.00	0.00** \pm 0.00	00.0
0.1 mM AgNPs	91.4 \pm 1.06	5.94 \pm 0.38	100.1
0.5 mM AgNPs	78.9** \pm 0.95	3.99** \pm 0.35	68.1
1.0 mM AgNPs	66.7** \pm 1.35	3.14** \pm 0.26	53.6

The values are means (M) of three replicates \pm standard deviation (SD). ** Significant at $P < 0.01$

noticeable reduction in the root length than shoot. Root growth of eleven wetland plants was more affected than leaf growth exposed to Ag^+ (Yin et al. 2012). In contrast, chemical AgNPs caused stronger inhibitory effect than Ag^+ on root length and fresh weight of *Arabidopsis thaliana* (Qian et al. 2013). Recently, faba bean seed germination declined by 40% in response to 800 μg AgNPs kg^{-1} soil, while the same level from Ag^+ completely inhibited seed germination of faba bean (Abd-Alla et al. 2016).

In the present study, the seedling shoot lengths of barley were reduced by 31.0 and 46.4% in response to 0.5 and 1 mM AgNPs, respectively, compared to the control

(Table 1). Vannini et al. (2014) reported that phytotoxic and genotoxic effects of AgNPs on wheat seedlings were primarily due to the release of Ag^+ from AgNPs. Also, rice germination and seedling growth were decreased with increasing sizes and concentrations of AgNPs (Thuesombat et al. 2014). However, El-Temsah and Joner (2012) reported that the seed germination inhibition of ryegrass, barley and flax was unaffected by the size of AgNPs.

In the present study, inhibition of barley grain germination and subsequent seedling growth increased with increasing concentration of Ag^+ and AgNPs treatments suggested both Ag^+ and AgNPs penetrated the grain parenchyma cells and transported to the embryo and seedling cells. Seed germination and root growth of different plant species were inhibited with NPs of Al, Zn, Al_2O_3 and ZnO (Lee et al. 2010; Lin and Xing 2007).

Determination of Ag content

Application of nanoparticles to soil and their uptake and accumulation in plants appear to be of great significance to explain the toxicity of nanoparticles in the environment. In the present study, leaves Ag concentrations showed a clear trend of increase with increasing AgNO_3 and AgNPs treatments compared to the untreated one (Table 2). Generally, Ag content of AgNO_3 treated barley leaves was much more than that treated with AgNPs. In details, leaves Ag contents increased by about 4 and 10 fold in response to 0.5 and 1 mM AgNO_3 treatments, respectively. In contrast, with 0.5 and 1 mM AgNPs treatments, the increase in Ag content of barley leaves were about 2 and 2.6 fold, respectively, compared to the control (Table 2). As a result, the absorption of silver ions (Ag^+) was more efficiently than AgNPs by leaf tissue. Our results indicated that the accumulation of Ag in barley leaves treated with AgNO_3 and AgNPs dependent on the dose concentration treatments and on silver forms (ion and particle). In this respect, Ma et al. (2010) and Qian et al. (2013) reported that the

Table 2 Ag concentration (mg kg^{-1} DW) of barley (*Hordeum vulgare* L. cv. Gustoe) leaves treated with Ag^+ or AgNPs (0.5 and 1 mM) for 3 weeks compared to the control

Treatments	Ag concentration (mg kg^{-1} DW)	
	M \pm SD	%
Control	1.82 \pm 0.23	100
0.5 mM AgNO_3	7.11** \pm 0.77	390
1.0 mM AgNO_3	18.16** \pm 1.76	999
0.5 mM AgNPs	3.72* \pm 0.78	204
1.0 mM AgNPs	4.75** \pm 0.51	261

The values are means (M) of three replicates \pm standard deviation (SD). * Significant at $P < 0.05$; ** Significant at $P < 0.01$

absorption and accumulation of AgNPs in the leaf tissue dependent on its diameter size and plant species. Moreover, AgNPs bioaccumulation factors of the root of *Phaseolus radiatus* and *Sorghum bicolor* were more than those of the leaves (Lee et al. 2012). Accumulation of Ag in *Potamogeton crispus* increased in a dose dependent manner and caused a considerable physiological, biochemical and ultrastructural changes (Xu et al. 2010).

Leaf morphology and cell ultrastructure

Leaves of control barley plants exhibited reflected normal morphology and they were dark green (Fig. 3). With increasing Ag⁺ and AgNPs treatments, the barley leaf chlorosis appeared after 7–12 d dependent on the dose and type of treatments. Leaf chlorosis was more evident with Ag⁺ treatments than AgNPs. Moreover, the chlorosis in plants treated with Ag⁺ was observed earlier than that treated with AgNPs. The severity of chlorosis and necrosis due to Ag⁺ and AgNPs was more visible in the tip and base of leaves.

Leaf ultrastructure observations of Ag⁺ (Fig. 5a–c) and AgNPs (Fig. 6a, b) treated barley showed higher subcellular disorganization compared to control plants (Fig. 4a, b). Chloroplasts of the control plants were lens to oval-shaped with a normal organization of inner structure. In contrast, destruction of inner structure of chloroplasts strongly occurred in response to Ag⁺-treated barley leaves (Fig. 5a–c). Ag⁺ (1 mM) treated leaves caused a

condensed stroma matrix of chloroplasts, formation of vesicles and dilated grana thylakoids. Grana thylakoids and stroma lamellae lost their organization. Chloroplasts contained a large size of plastoglobuli compared with that of the control. Our results concerning the destruction of chloroplasts under effect of Ag⁺ and Ag NPs correspond with that reported by Qian et al. (2013), they reported that Ag⁺ and AgNPs disrupted the thylakoid membrane structure and decreased chlorophyll content in *Arabidopsis thaliana*. In response to 1 mM of Ag⁺, the mitochondrial envelope and cristae was partially or totally degenerated (Fig. 5b). Damage of mitochondria structure in response to Ag⁺ and AgNPs may lead to physiological dysfunction. In this respect, increasing AgNPs exposure in rice root seedlings decreased mitochondrial membrane potential (Nair and Chung 2014). Nucleus of the control had normal distribution of nuclear materials. Ag⁺-treated barley caused clumping of nuclear chromatin into more densely packed material, probably, as result of oxidative stress effect (Fig. 5c). On the molecular level, Ag⁺ and AgNPs led to upregulation and downregulation of genes in *Arabidopsis thaliana* (Kaveh et al. 2013) and in *Eruca sativa* (Vannini et al. 2013). In response to AgNPs treatments, the chloroplasts (Fig. 6a) had well defined grana thylakoids and stroma lamellae, but there was a reduction in size of grana thylakoids to stroma lamellae (Fig. 6b). Chloroplasts of AgNPs-treated barley have small and few numbers of plastoglobuli compared to that treated with Ag⁺. Due to AgNPs treatment, nuclear envelope was ruptured and small particles have the same morphology and size spread in the nucleus and cytoplasm (Fig. 6a). Ag accumulation in Ag⁺-treated barley leaves was higher than that treated with AgNPs, probably a reason, which caused a severe misshaped in the cell organelles.

Photosynthetic pigments

The negative action of Ag⁺ on barley probably results from its influence on photosynthetic pigments in plants. Chl *a*, chl *b* and carotenoids contents of barley leaves were significantly decreased with Ag⁺ and AgNPs applications compared to the control (Table 3). The decrease in pigment contents was higher with Ag⁺ treatments than that treated with AgNPs. For example, chl *a* content decreased by 25.4 and 35.6% in response to 0.5 and 1.0 mM of Ag⁺, respectively, while the chl *a* decreased by 13.7 and 24% in response to 0.5 and 1.0 mM AgNPs treatments, respectively, compared with the control. The chl *b* contents of barley leaves significantly decreased with increasing Ag⁺ and AgNPs treatments (Table 3). Due to 0.5 and 1.0 mM of Ag⁺ treatments, the chl *b* decreased by 31.8 and 40.9%, respectively, compared to the control. While with 0.5 and 1.0 mM of AgNPs treatments, the chl *b* decreased by 13.6

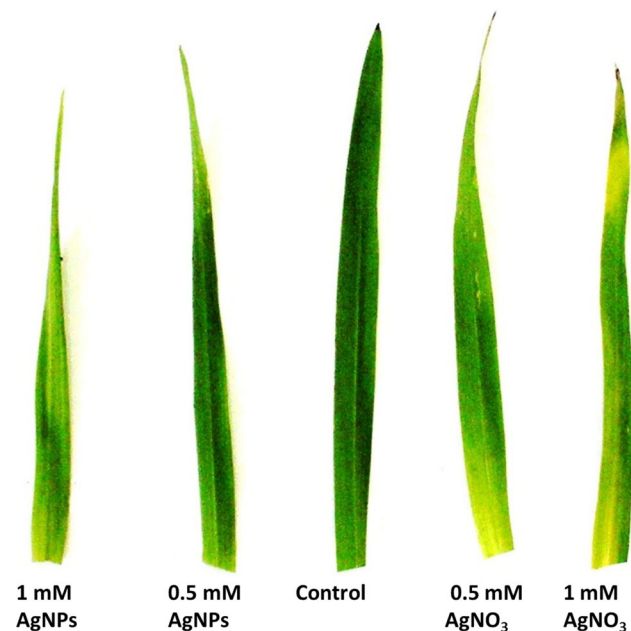


Fig. 3 Leaf morphology of barley (*Hordeum vulgare* L. cv. Gustoe) treated with two concentrations of AgNO₃ and AgNPs (0.5 and 1 mM) for 3 weeks

Fig. 4 Untreated mesophyll cells (a) and chloroplast (b) of barley leaves (*Hordeum vulgare* L. cv. Gustoe). C chloroplast, CW cell wall, G granum, N nucleus. Scale bars 500 nm (a) and 200 nm (b)

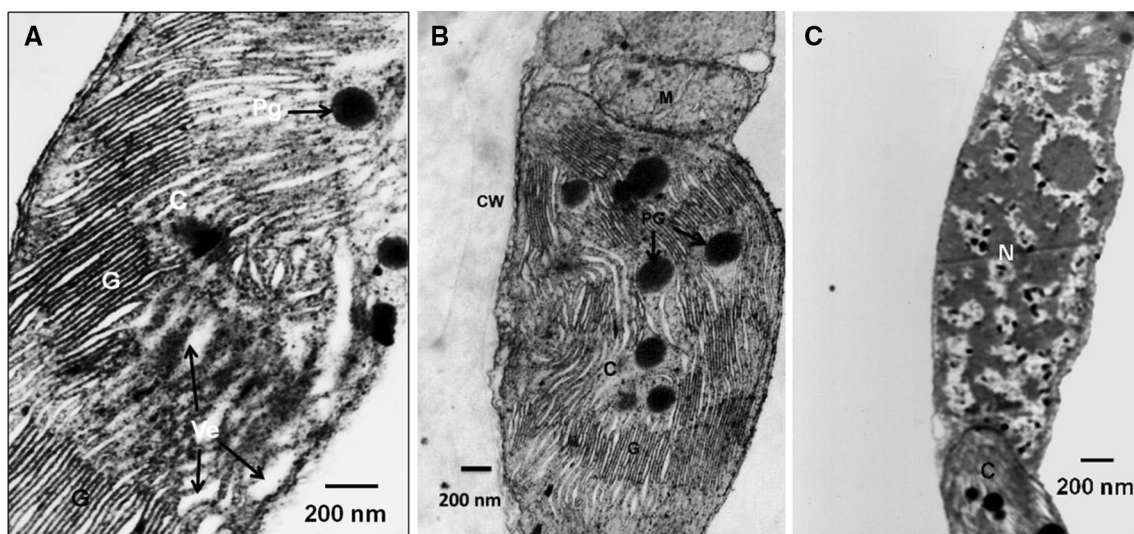
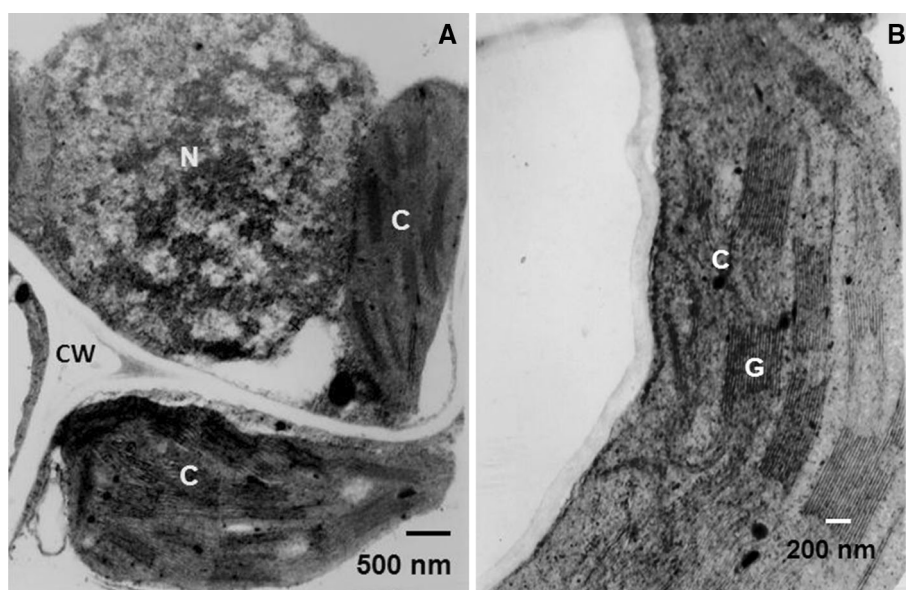


Fig. 5 Mesophyll cell (a), chloroplast (b) and nucleus (c) of barley leaves (*Hordeum vulgare* L. cv. Gustoe) treated with 1 mM AgNO_3 for 3 weeks. C chloroplast, CW cell wall, G granum, N nucleus, Pg plastoglobuli, Ve vesicle. Scale bars 200 nm (a), 200 nm (b) and 200 nm (c)

and 29.6%, respectively. The chl *b* content, in most cases, decreased more than chl *a* content in response to Ag^+ and AgNPs treatments and it caused an increase in the chl *a/b* ratio suggesting that the chl *b* is highly sensitive than chl *a* to Ag^+ and AgNPs action. AgNPs declined chlorophyll fluorescence (Falco et al. 2015). It is possible that the aldehyde group (reducing group) of chl *b* is more sensitive than that of methyl group of chl *a* to reacts with ROS that formed due to Ag^+ and AgNPs treatments. Carotenoid contents of barley decreased under effect of Ag^+ and AgNPs treatments and the most decrease in carotenoid content occurred at 1.0 mM Ag^+ treatments (67.3% of the control). Chlorophyll contents of plants decreased under

effect of salinity and drought stresses (Fayez and Bazaid 2014; Shaddad et al. 1988). In this work, the total pigment contents of barley leaves were lowered in a dose dependent manner, mostly with 1 mM of Ag^+ . The reduction of photosynthetic pigments, damage of chloroplasts and other cell organelles of barley due to Ag effect are comparable to those occurred in plants under effect of other environmental stresses (Fayez 2000; Fayez and Abd-Elfattah 2007; Fayez and Mahmoud 2011; Fayez et al. 2014; Manios et al. 2003; Oukarroum et al. 2012). From the results herein, we suggest that the decline in photosynthetic pigments contents of barley leaves could be attributed to the toxicity of Ag as AgNPs form.

Fig. 6 Mesophyll cells (a) and chloroplast (b) of barley leaves (*Hordeum vulgare* L. cv. Gustoe) treated with 1 mM AgNPs for 3 weeks. Small vesicles in chloroplast (arrows), rupture of nuclear envelope (asterisk), and small particles have the same morphology and size (arrow heads) spread in the nucleus and cytoplasm were observed (a). C chloroplast, CW cell wall, G granum, M mitochondrion, N nucleus, Pg plastoglobuli, SL stroma lamellae, V vacuole. Scale bars 500 nm (a) and 200 nm (b)

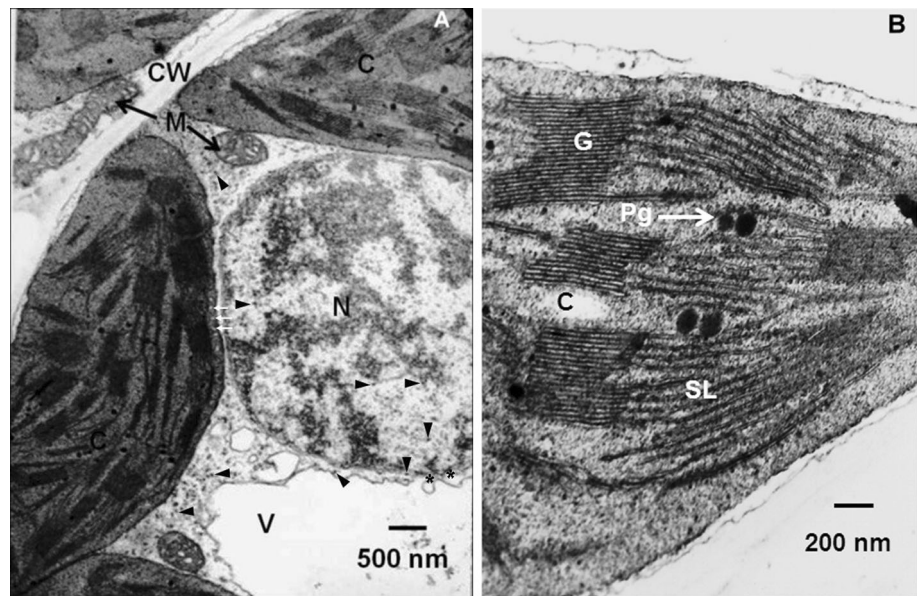


Table 3 Photosynthetic pigment contents (mg g^{-1} FW) of barley (*Hordeum vulgare* L. cv. Gustoe) leaves treated with Ag^+ or AgNPs (0.5 and 1 mM) for 3 weeks compared to the control

Treatments	Chl <i>a</i>		Chl <i>b</i>		Carotenoids		<i>alb</i> ratio	Total	%
	M \pm SD	%	M \pm SD	%	M \pm SD	%			
Control	1.46 \pm 0.17	100	0.44 \pm 0.04	100	0.55 \pm 0.13	100	3.32	2.45	100
0.5 mM AgNO_3	1.09* \pm 0.10	74.6	0.30** \pm 0.03	68.2	0.44 \pm 0.04	80.0	3.63	1.83	74.7
1.0 mM AgNO_3	0.94** \pm 0.09	64.4	0.26** \pm 0.02	59.1	0.37** \pm 0.03	67.3	3.62	1.57	64.1
0.5 mM AgNPs	1.26 \pm 0.10	86.3	0.38** \pm 0.03	86.4	0.47 \pm 0.05	85.4	3.32	2.11	86.1
1.0 mM AgNPs	1.11* \pm 0.08	76.0	0.31** \pm 0.03	70.4	0.43 \pm 0.03	78.2	3.58	1.85	75.5

The values are means (M) of three replicates \pm standard deviation (SD). * Significant at $P < 0.05$; ** Significant at $P < 0.01$

Malondialdehyde content

The oxidation products of lipid and protein are considered as indicator of oxidative stress biomarkers in stressed plants (Anjum et al. 2015; Barbasz et al. 2016). Malondialdehyde (MDA) content of barley leaves was declined by 23% due to 0.5 mM of Ag^+ compared to the control. In contrast, under effect of 1 mM of Ag^+ , MDA content of barley leaves increased by 25.7% compared to the control (Fig. 7). MDA content in AgNPs-treated leaves was higher than in leaves treated with Ag^+ . In comparison to the control, leaf MDA contents increased by 107 and 76.2% in response to 0.5 and 1.0 mM AgNPs treatments, respectively. Nanoparticles of TiO_2 , CuO and ZnO induced lipid peroxidation in algae (Aruoja et al. 2009; Chen et al. 2012). Free radicals attack such as reactive oxygen species (ROS) cause lipid peroxidation in biological organisms (Sevanian and Ursini 2000). Free Ag^+ increased ROS and frond abscission in *Lemna gibba* (Oukarroum et al. 2013). Increasing AgNPs exposure caused increase in reactive

oxygen species generation and cytotoxicity in rice root seedlings (Nair and Chung 2014). The elevated levels of MDA in plants due to metal ions or particles was resulted from the stimulation of free radical-generating capacity of the plant, however, lower MDA level in the cells was observed with the long-term exposure of high concentration of cadmium (Chen et al. 2014). We suggest that the elevated MDA levels was not only due to the presence of Ag^+ but also to the AgNPs.

Soluble proteins and total phenolic compounds contents

Soluble proteins (Table 4) of barley leaves were significantly increased in response to Ag^+ and AgNPs treatments. In response to 0.5 and 1.0 mM of Ag^+ , the soluble proteins content increased by 11 and 31%, respectively, compared to the control. On the other hand, 0.5 and 1.0 mM of AgNPs increased soluble proteins by 53 and 39%, respectively. Changes of soluble proteins with various

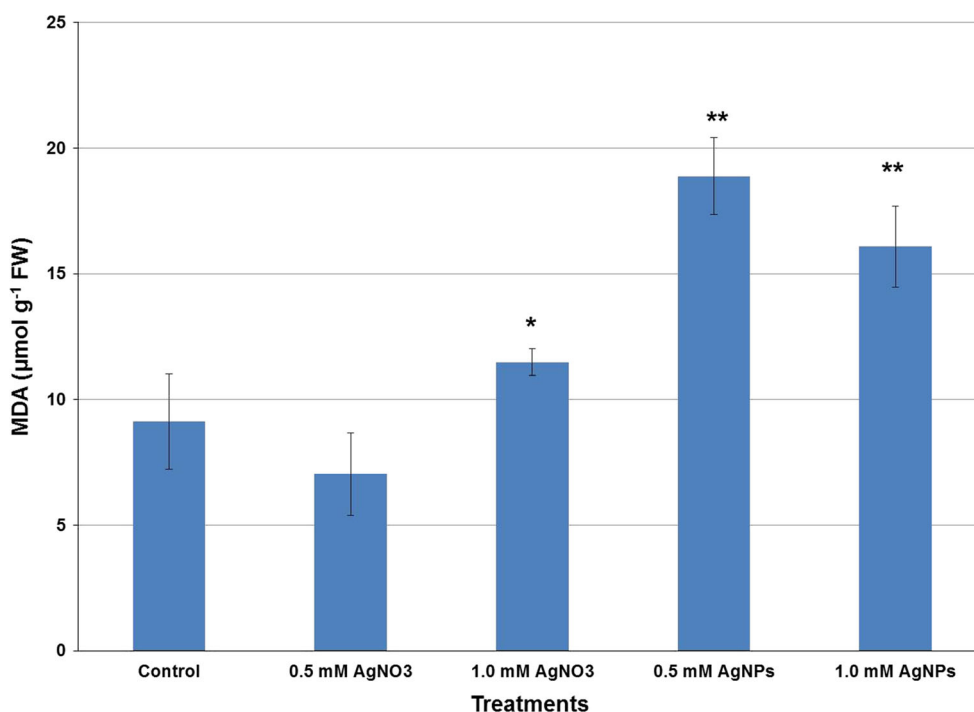


Fig. 7 MDA content of barley leaves (*Hordeum vulgare* L. cv. Gustoe) treated with the two concentrations of AgNO₃ and AgNPs (0.5 and 1 mM) for 3 weeks. The values are means (M) of three replicates \pm standard deviation (SD). *Significant at $P < 0.05$; **Significant at $P < 0.01$

Table 4 Soluble protein contents (mg g⁻¹ DW) and total phenolic (µg gallic acid g⁻¹ DW) of barley (*Hordeum vulgare* L. cv. Gustoe) leaves treated with Ag⁺ or AgNPs (0.5 and 1 mM) for 3 weeks compared to the control

Treatments	Soluble protein (mg g ⁻¹ DW)		Total phenolic (µg gallic acid g ⁻¹ DW)	
	M \pm SD	%	M \pm SD	%
Control	22.65 \pm 1.67	100	47.13 \pm 2.82	100
0.5 mM AgNO ₃	25.17 \pm 1.55	111	57.60** \pm 3.83	122
1.0 mM AgNO ₃	29.64** \pm 1.04	131	61.82** \pm 2.28	130
0.5 mM AgNPs	34.63** \pm 3.94	153	71.43** \pm 4.21	152
1.0 mM AgNPs	31.57** \pm 3.31	139	77.75** \pm 4.20	165

The values are means (M) of three replicates \pm standard deviation (SD). ** Significant at $P < 0.01$

abiotic stresses were reported (Fayez and Bazaid 2014; Fayez et al. 2014). As per the suggestion of Zheng et al. (2009), the increasing soluble proteins content under effect of Ag⁺ and AgNPs was related to metal tolerance in plant.

Phenolic compounds are widely distributed in the plant kingdom. Some phenolic compounds in living organisms are involved in resistance to environmental stresses (Delalonde et al. 1996). All treatments of Ag⁺ and AgNPs used in the experiment showed an increase in leaf phenolic compounds compared to control plants (Table 4). Moreover, with increasing Ag⁺ and AgNPs treatments, the leaf total phenolic compounds gradually increased. Leaf phenolic contents of the control, 0.5 and 1 mM Ag⁺ were 47.13, 57.60 and 61.82 µg g⁻¹ DW, respectively. Due to application of 0.5 and 1 mM AgNPs, leaf phenolic contents were 71.13 µg g⁻¹ DW (152% of the control) and

77.75 µg g⁻¹ DW (165% of the control), respectively. These responses were reported in plants under heavy metal stress (Sakihama et al. 2002; Sytar et al. 2013). The significance of phenolic compounds in the protection of Ag⁺ and AgNPs-mediated oxidative stress has been evidenced (Krishnaraj et al. 2012; Yasur and Rani 2013).

Peroxidase activity

Oxidative stress defined as a change in the equilibrium between oxidant and antioxidant activities. Analysis of guaiacol antioxidant enzyme (POD) showed considerable different changes in its activity upon supply of Ag⁺ and AgNPs compared to the control (Table 5). The POX activity of barley leaves significantly increased due to Ag⁺ treatments. In response to 0.5 and 1.0 mM of Ag⁺, the

Table 5 Guaiacol peroxidase (POX) activity (U g⁻¹ FW) of barley (*Hordeum vulgare* L. cv. *Gustoe*) leaves treated with Ag⁺ or AgNPs (0.5 and 1 mM) for 3 weeks compared to the control

Treatments	POX activity (U g ⁻¹ FW)	
	M ± SD	%
Control	181.05 ± 21.70	100
0.5 mM AgNO ₃	219.50* ± 18.71	121.2
1.0 mM AgNO ₃	229.11** ± 15.22	126.5
0.5 mM AgNPs	256.26** ± 22.73	141.5
1.0 mM AgNPs	186.69 ± 26.02	103.1

The values are means (M) of three replicates ± standard deviation (SD). * Significant at $P < 0.05$; ** significant at $P < 0.01$

POX activities increased by 21.2 and 26.5%, respectively, compared to the control. In response to 0.5 mM AgNPs, the POX activity increased by 41.5% compared to the control. However, with 1 mM AgNPs treatment, the POX activity was approximately equal to that of the control.

Metals increased ROS generation within cellular resulted in an oxidative damage (Bartosz 1997). ROS production was observed in *Chlamydomonas reinhardtii* due to indirect influence of the high affinity of Ag⁺ to thiol groups (Szivák et al. 2009). Herein, Ag⁺ and AgNPs changed the balance between the oxidant and antioxidant systems in the barley leaves. Ag⁺ and AgNO₃ caused oxidative damage as evidenced by inhibition of grain germination, seedling growth, damage of leaf cell organelles, decreased chlorophyll content and increased lipid peroxidation. However, MDA content (Fig. 7) and peroxidase activity (Table 5) of barley leaves at 1 mM AgNPs treated plants were lower than that of 0.5 mM AgNPs, which implied other antioxidants involved in the cell detoxification. In this respect, we found that the total phenolic compounds (one of the antioxidant compounds) of barley leaves had the highest value at 1 mM AgNPs (Table 4). Therefore, further studies are required to investigate the activities of other antioxidants and oxidative stress with Ag⁺ and AgNPs applications.

Conclusions

Our results showed that the seed germination, seedling lengths, leaf cell organelles, photosynthetic pigments, lipid peroxidation, soluble proteins, total phenolic compounds and peroxidase activity of barley were seriously affected by Ag⁺ and AgNPs treatments. Accumulation of Ag in the barley leaves was dependent on the concentration of Ag⁺ and AgNPs dose applications and on the silver forms (ions or particles). Ag⁺ effect was more noticeable than AgNPs on barley grain germination and seedling growth. Root

growth was more seriously affected by Ag⁺ and AgNPs than shoot. Leaf chlorosis induced by Ag⁺ and AgNPs resulted from the decrease in chlorophyll contents. Consequently, decreased photosynthetic pigment contents and increased MDA content in response to effect of Ag⁺ and AgNPs provided evidences on the enhancement of oxidative stress. Damage of chloroplasts, mitochondria and nucleus ultrastructure confirmed that these organelles were the main targets affected by Ag toxicity.

Author contribution statement KAF did the experiments of germination, cultivation, ultrastructure and physiological activities of barley plant and wrote the manuscript; BAE-D did the biosynthesis of silver nanoparticles; NYM did the characterizations of silver nanoparticles and silver determination in barley leaves. The three authors have read and approved the final manuscript.

Acknowledgements The project was funded by the University Research Projects (1-434-2623), Taif University, Saudi Arabia.

References

- Abd-Alla MH, Nafady NA, Khalaf DM (2016) Assessment of silver nanoparticles contamination on faba bean-*Rhizobium leguminosarum* bv. *viciae-Glomus aggregatum* symbiosis: Implications for induction of autophagy process in root nodule. *Agric Ecosyst Environ* 218:163–177
- Al-Harbi M, El-Deeb B, Mostafa N, Amer S (2014) Extracellular biosynthesis of AgNPs by the bacterium *Proteus mirabilis* and its toxic effect on some aspects of animal physiology. *Adv Nanoparticl* 3:83–91
- American Society for Testing and Materials (2006) Standard terminology relating to nanotechnology. E 2456-06. West Conshohocken PA
- Amooghaie R, Saeri MR, Azizi M (2015) Synthesis characterization and biocompatibility of silver nanoparticles synthesized from *Nigella sativa* leaf extract in comparison with chemical silver nanoparticles. *Ecotoxicol Environ Saf* 120:400–408
- Anjum N, Sofo A, Scopa A, Roychoudhury A, Gill S, Iqbal M, Lukatkin A, Pereira E, Duarte A, Ahmad I (2015) Lipids and proteins-major targets of oxidative modifications in abiotic stressed plants. *Environ Sci Pollut Res* 22:4099–4121
- Aruoja V, Dubourguie H, Kasemets K, Kahru A (2009) Toxicity of nanoparticles of CuO, ZnO and TiO₂ to microalgae *Pseudokirchneriella subcapitata*. *Sci Total Environ* 407:1461–1468
- Barbasz A, Kreczmer B, Oćwieja M (2016) Effects of exposure of callus cells of two wheat varieties to silver nanoparticles and silver salt (AgNO₃). *Acta Physiol Plant* 38:1–11
- Bartosz G (1997) Oxidative stress in plants. *Acta Physiol Plant* 19:47–64
- Battke F, Leopold K, Maier M, Schmidhalter U, Schuster M (2008) Palladium exposure of barley: uptake and effects. *Plant Biol* 10:272–276
- Bhainsa KC, D'Souza SF (2006) Extracellular biosynthesis of silver nanoparticles using the fungus *Aspergillus fumigatus*. *Colloids Surf B: Biointerfaces* 47:160–164
- Chairuangkitti P, Lawanprasert S, Roytrakul S, Aueviriyavit S, Phummiratch D, Kulthong K, Chanvorachote P,

- Maniratanachote R (2013) Silver nanoparticles induce toxicity in a549 cells via ROS-dependent and ROS-independent pathways. *Toxicol In Vitro* 27:330–338
- Chen L, Zhou L, Liu Y, Deng S, Wu H, Wang G (2012) Toxicological effects of nanometer titanium dioxide (nano-TiO₂) on *Chlamydomonas reinhardtii*. *Ecotoxicol Environ Saf* 84:155–162
- Chen A, Zeng G, Chen G, Liu L, Shang C, Hu X, Lu L, Chen M, Zhou Y, Zhang Q (2014) Plasma membrane behavior, oxidative damage, and defense mechanism in *Phanerochaete chrysosporium* under cadmium stress. *Process Biochem* 49:589–598
- Choi O, Hu Z (2008) Size dependent and reactive oxygen species related nanosilver toxicity to nitrifying bacteria. *Environ Sci Technol* 42:4583–4588
- Cvjetko P, Milošić A, Domijan A-M, Vinković Vrček I, Tolić S, Peharec Štefanić P, Letofsky-Papst I, Tkalec M, Balen B (2017) Toxicity of silver ions and differently coated silver nanoparticles in *Allium cepa* roots. *Ecotoxicol Environ Saf* 137:18–28
- Dai GH, Andary C, Cosson-Monodol L, Boubals D (1994) Polyphenols and resistance of grapevines to downy mildew. *Acta Horticult* 381:763–766
- Delalonde M, Barret Y, Coumans MP (1996) Development of phenolic compounds in maize anthers (*Zea mays*) during cold pretreatment prior to androgenesis. *J Plant Physiol* 149:612–616
- Dietz K-J, Herth S (2011) Plant nanotoxicology. *Trends Plant Sci* 16:582–589
- Doshi R, Braidia W, Christodoulatos C, Wazne M, O'Connor G (2008) Nano-aluminum: Transport through sand columns and environmental effects on plants and soil communities. *Environ Res* 106:296–303
- Dubey P, Matai I, Kumar SU, Sachdev A, Bhushan B, Gopinath P (2015) Perturbation of cellular mechanistic system by silver nanoparticle toxicity: cytotoxic, genotoxic and epigenetic potentials. *Adv Colloid Interface Sci* 221:4–21
- El-Temsah YS, Joner EJ (2012) Impact of Fe and Ag nanoparticles on seed germination and differences in bioavailability during exposure in aqueous suspension and soil. *Environ Toxicol* 27:42–49
- Fabrega J, Luoma SN, Tyler CR, Galloway TS, Lead JR (2011) Silver nanoparticles: behaviour and effects in the aquatic environment. *Environ Int* 37:517–531
- Falco WF, Queiroz AM, Fernandes J, Botero ER, Falcão EA, Guimarães FEG, M'Peko JC, Oliveira SL, Colbeck I, Caires ARL (2015) Interaction between chlorophyll and silver nanoparticles: a close analysis of chlorophyll fluorescence quenching. *J Photochem Photobiol A Chem* 299:203–209
- Fayez KA (2000) Action of photosynthetic diuron herbicide on cell organelles and biochemical constituents of the leaves of two soybean cultivars. *Pest Biochem Physiol* 66:105–115
- Fayez KA, Abd-Elfattah Z (2007) Alteration in growth and physiological activities in *Chlorella vulgaris* under the effect of photosynthetic inhibitor diuron. *Inter J Agri Biol* 9:631–634
- Fayez KA, Bazaid SA (2014) Improving drought and salinity tolerance in barley by application of salicylic acid and potassium nitrate. *J Saudi Soc Agric Sci* 13:45–55
- Fayez KA, Mahmoud SY (2011) Detection and partial characterization of a putative closterovirus affecting *Ficus carica*: molecular ultrastructural and physiological aspects of infected leaves. *Acta Physiol Plant* 33:2187–2198
- Fayez KA, Radwan DEM, Mohamed AK, Abdelrahman AM (2014) Fusilade herbicide causes alterations in chloroplast ultrastructure pigment content and physiological activities of peanut leaves. *Photosynthetica* 52:548–554
- Godin B, Sakamoto JH, Serda RE, Grattoni A, Bouamrani A (2010) Emerging applications of nanomedicine for the diagnosis and treatment of cardiovascular diseases. *Trends Pharmacol Sci* 31:199–205
- Gorczyca A, Pocięcha E, Kasprówicz M, Niemiec M (2015) Effect of nanosilver in wheat seedlings and *Fusarium culmorum* culture systems. *Eur J Plant Pathol* 142:251–261
- Gurunathan S, Kalishwaralal K, Vaidyanathan R, Venkataraman D, Pandian SRK, Muniyandi J, Hariharan N, Eom SH (2009) Biosynthesis purification and characterization of silver nanoparticles using *Escherichia coli*. *Colloids Surf B: Biointerfaces* 74:328–335
- Hassan FAS, Ali EF, El-Deeb BA (2014) Improvement of postharvest quality of cut rose cv. 'First Red' by biologically synthesized silver nanoparticles. *Sci Hortic* 179:340–348
- Haverkamp RG, Marshall AT (2009) The mechanism of metal nanoparticle formation in plants: limits on accumulation. *J Nanopart Res* 11:1453–1463
- Hernández JA, Almansa MS (2002) Short-term effects of salt stress on antioxidant systems and leaf water relations of pea leaves. *Physiol Plant* 115:251–257
- Hood E (2004) Nanotechnology: looking as we leap. *Environ Health Perspect* 112:A740–A749
- Impellitteri CA, Tolaymat TM, Scheckel KG (2009) The speciation of silver nanoparticles in antimicrobial fabric before and after exposure to a hypochlorite/detergent solution. *J Environ Qual* 38:1528–1530
- Kaveh R, Li YS, Ranjbar S, Tehrani R, Brueck CL, Van Aken B (2013) Changes in *Arabidopsis thaliana* gene expression in response to silver nanoparticles and silver ions. *Environ Sci Technol* 18:10637–10644
- Kim JS, Kuk E, Yu KN, Kim JH, Park SJ, Lee HJ, Cho MH (2007) Antimicrobial effects of silver nanoparticles. *Nanomed Nanotechnol Biol Med* 3:95–101
- Klaine SJ, Alvarez PJJ, Batley GE, Fernandes TF, Handy RD, Lyon DY, Mahendra S, McLaughlin MJ, Lead JR (2008) Nanomaterials in the environment: behavior fate bioavailability and effects. *Environ Toxicol Chem* 27:1825–1851
- Kokura S, Handa O, Takagi T, Ishikawa T, Naito Y, Yoshikawa T (2010) Silver nanoparticles as a safe preservative for use in cosmetics. *Nanomed Nanotechnol Biol Med* 6:570–574
- Krishnaraj C, Jagan EG, Ramachandran R, Abirami SM, Mohan N, Kalaichelvan PT (2012) Effect of biologically synthesized silver nanoparticles on *Bacopa monnieri* (Linn.) Wettst. plant growth metabolism. *Process Biochem* 47:651–658
- Kumar V, Yadav SK (2009) Plant-mediated synthesis of silver and gold nanoparticles and their applications. *J Chem Technol* 84:151–157
- Kumari M, Mukherjee A, Chandrasekaran N (2009) Genotoxicity of silver nanoparticles in *Allium cepa*. *Sci Tot Environ* 407:5243–5246
- Lee CW, Mahendra S, Zodrow K, Li D, Tsai Y-C, Braam J, Alvarez PJJ (2010) Developmental phytotoxicity of metal oxide nanoparticles to *Arabidopsis thaliana*. *Environ Toxicol Chem* 29:669–675
- Lee W-M, Kwak JI, An Y-J (2012) Effect of silver nanoparticles in crop plants *Phaseolus radiatus* and *Sorghum bicolor*: media effect on phytotoxicity. *Chemosphere* 86:491–499
- Lichtenthaler HK (1987) Chlorophylls and carotenoids—pigments of photosynthetic biomembranes. In: Colowick SP, Kaplan NO (eds) *Methods in enzymology*, vol 148. Academic Press, San Diego, pp 350–382
- Lin DH, Xing BS (2007) Phytotoxicity of nanoparticles: inhibition of seed germination and root growth. *Environ Pollut* 150:243–250
- Lowry OH, Rosebrough NJ, Farr AI, Randall RJ (1951) Protein measurement with the folin phenol reagent. *J Biol Chem* 193:291–297
- Lü P, Cao J, He S, Liu J, Li H, Cheng G, Ding Y, Joyce DC (2010) Nano-silver pulse treatments improve water relations of cut rose cv. Movie Star flowers. *Postharvest Biol Technol* 57:196–202

- Luft JH (1961) Improvements in epoxy embedding methods. *J Biophys Biochem Cytol* 9:409–414
- Ma X, Geiser-Lee J, Deng Y, Kolmakov A (2010) Interactions between engineered nanoparticles (ENPs) and plants: phytotoxicity uptake and accumulation. *Sci Total Environ* 408:3053–3061
- Manios T, Stentiford EI, Millner PA (2003) The effect of heavy metals accumulation on the chlorophyll concentration of *Typha latifolia* plants growing in a substrate containing sewage sludge compost and watered with metaliferous water. *Ecol Eng* 20:65–74
- Marambio-Jones C, Hoek EM (2010) A review of the antibacterial effects of silver nanomaterials and potential implications for human health and the environment. *J Nanopart Res* 12:1531–1551
- Mazumdar H, Ahmed GU (2011) Phytotoxicity effect of silver nanoparticles on *Oryza sativa*. *Inter J Chem Tech Res* 3:1494–1500
- McGillicuddy E, Murray I, Kavanagh S, Morrison L, Fogarty A, Cormican M, Dockery P, Prendergast M, Rowan N, Morris D (2017) Silver nanoparticles in the environment: sources, detection and ecotoxicology. *Sci Total Environ* 575:231–246
- Miao AJ, Schwehr KA, Xu C, Zhang SJ, Luo Z, Quigg A, Santschi PH (2009) The algal toxicity of silver engineered nanoparticles and detoxification by exopolymeric substances. *Environ Pollut* 157:3034–3041
- Mulvaney P (1996) Surface plasmon spectroscopy of nanosized metal particles. *Langmuir* 12:788–800
- Musante C, White JC (2012) Toxicity of silver and copper to *Cucurbita pepo*: differential effects of nano and bulk-size particles. *Environ Toxicol* 27:510–517
- Nair PMG, Chung IM (2014) Physiological and molecular level effects of silver nanoparticles exposure in rice (*Oryza sativa* L.) seedlings. *Chemosphere* 112:105–111
- Navarro E, Baun A, Behra R, Hartmann N, Filser J, Miao A-J, Quigg A, Santschi P, Sigg L (2008a) Environmental behavior and ecotoxicity of engineered nanoparticles to algae plants and fungi. *Ecotoxicology* 17:372–386
- Navarro E, Piccapietra F, Wagner B, Marconi F, Kaegi R, Odzak N, Sigg L, Behra R (2008b) Toxicity of silver nanoparticles to *Chlamydomonas reinhardtii*. *Environ Sci Technol* 42:8959–8964
- Nel A, Xia T, Madler L, Li N (2006) Toxic potential of materials at the nanolevel. *Science* 311:622–627
- Oukarroum A, Bras S, Perreault F, Popovic R (2012) Inhibitory effects of silver nanoparticles in two green algae, *Chlorella vulgaris* and *Dunaliella tertiolecta*. *Ecotoxicol Environ Saf* 78:80–85
- Oukarroum A, Gaudreault M-H, Pirastru L, Popovic R (2013) Alleviation of silver toxicity by calcium chloride (CaCl₂) in *Lemna gibba* L. *Plant Physiol Biochem* 71:235–239
- Pal S, Tak YK, Song JM (2007) Does the antibacterial activity of silver nanoparticles depend on the shape of the nanoparticle? A study of the gram-negative bacterium *Escherichia coli*. *Appl Environ Microbiol* 73:1712–1720
- Polle A, Otter T, Seifert F (1994) Apoplastic peroxidases and lignification in needles of Norway spruce (*Picea abies* L.). *Plant Physiol* 106:53–60
- Qian H, Peng X, Han X, Ren J, Sun L, Fu Z (2013) Comparison of the toxicity of silver nanoparticles and silver ions on the growth of terrestrial plant model *Arabidopsis thaliana*. *J Environ Sci* 25:1947–1956
- Rajan A, Vilas V, Philip D (2015) Catalytic and antioxidant properties of biogenic silver nanoparticles synthesized using *Areca catechu* nut. *J Mol Liq* 207:231–236
- Rasband WS (1997) Image U.S. National Institutes of Health Bethesda Maryland USA. <http://imagej.nih.gov/ij/>
- Raut R, Kolekar N, Lakkakula J, Mendhulkar V, Kashid S (2010) Extracellular synthesis of silver nanoparticles using dried leaves of *Pongamia pinnata* (L) pierre. *Nano-Micro Lett* 2:106–113
- Sakihama Y, Cohen MF, Grace SC, Yamasaki H (2002) Plant phenolic antioxidant and prooxidant activities: phenolics-induced oxidative damage mediated by metals in plants. *Toxicology* 177:67–80
- Sevanian A, Ursini F (2000) Lipid peroxidation in membranes and low-density lipoproteins: similarities and differences. *Free Radical Biol Med* 29:306–311
- Shaddad MA, Ahmed AM, Fayez KA (1988) Alleviation of the adverse effects of salinity by nitrogen fertilization. *Biol Plant* 30:343–350
- Shaligram NS, Bule M, Bhambure R, Singhal RS, Singh SK, Szakacs G, Pandey A (2009) Biosynthesis of silver nanoparticles using aqueous extract from the compactin producing fungal strain. *Process Biochem* 44:939–943
- Sharma VK, Yngard RA, Lin Y (2009) Silver nanoparticles: green synthesis and their antimicrobial activities. *Adv Colloid Interface Sci* 145:83–96
- Shivaji S, Madhu S, Singh S (2011) Extracellular synthesis of antibacterial silver nanoparticles using psychrophilic bacteria. *Process Biochem* 46:1800–1807
- Sytar O, Cai Z, Brestic M, Kumar A, Prasad MNV, Taran N, Smetanska I (2013) Foliar applied nickel on buckwheat (*Fagopyrum esculentum*) induced phenolic compounds as potential antioxidants. *Clean-Soil Air Water* 41:1129–1137
- Szivák I, Behra R, Sigg L (2009) Metal-induced reactive oxygen species production in *Chlamydomonas reinhardtii* (Chlorophyceae). *J Phycol* 45:427–435
- Thuesombat P, Hannongbua S, Akasit S, Chadchawan S (2014) Effect of silver nanoparticles on rice (*Oryza sativa* L. cv. KDML 105) seed germination and seedling growth. *Ecotoxicol Environ Saf* 104:302–309
- Tiede K, Boxall ABA, Tear SP, Lewis J, David H, Hassellöv M (2008) Detection and characterization of engineered nanoparticles in food and the environment. *Food Addit Contam* 25:795–821
- Vannini C, Domingo G, Onelli E, Prinsi B, Marsoni M, Espen L, Bracale M (2013) Morphological and proteomic responses of *Eruca sativa* exposed to silver nanoparticles or silver nitrate. *PLoS ONE* 8:e68752
- Vannini C, Domingo G, Onelli E, De Mattia F, Bruni I, Marsoni M, Bracale M (2014) Phytotoxic and genotoxic effects of silver nanoparticles exposure on germinating wheat seedlings. *J Plant Physiol* 171:1142–1148
- Xu QS, Hu JZ, Xie KB, Yang HY, Du KH, Shi GX (2010) Accumulation and acute toxicity of silver in *Potamogeton crispus* L. *J Hazard Mater* 173:186–193
- Yasur J, Rani P (2013) Environmental effects of nanosilver: impact on castor seed germination seedling growth and plant physiology. *Environ Sci Pollut Res* 20:8636–8648
- Yin L, Cheng Y, Espinasse B, Colman BP, Auffan M, Wiesner M, Rose J, Liu J, Bernhardt ES (2011) More than the ions: the effects of silver nanoparticles on *Lolium multiflorum*. *Environ Sci Technol* 45:2360–2367
- Yin L, Colman BP, McGill BM, Wright JP, Bernhardt ES (2012) Effects of silver nanoparticle exposure on germination and early growth of eleven wetland plants. *PLoS One* 7:47674
- Yuan Z, Li J, Cui L, Xu B, Zhang H, Yu C-P (2013) Interaction of silver nanoparticles with pure nitrifying bacteria. *Chemosphere* 90:1404–1411
- Zheng W, Fei Y, Huang Y (2009) Soluble protein and acid phosphatase exuded by ectomycorrhizal fungi and seedlings in response to excessive Cu and Cd. *J Environ Sci* 21:1667–1672